# From Ringdowns to Critical Points: Constraining Dense Matter with Neutron Stars

Christian Ecker

Second Holography and Dense Matter Workshop
APC Laboratory Paris, 18 September 2025

Based on Nature Commun. 16 (2025) 1, 1320 (2403.03246) with
Tyler Gorda, Aleksi Kurkela and Luciano Rezzolla

and (2506.10065) with Niko Jokela and Matti Järvinen

# Motivation

**Two closely related challenges:**

- QCD phase diagram and the dense matter equation of state (EOS).
- Interior composition and properties of neutron stars and their mergers.

**Approach:** Dense matter theory + simulation + astro-observation.

- **Part 1:** Model-agnostic EOSs + simulations of long-ringdown slope.
  CE, Gorda, Kurkela, Rezzolla 2403.03246 (Nature Commun.)
- **Part 2:** Critical endpoint inference with V-QCD and astro-input.
  CE, Jokela, Järvinen 2506.10065

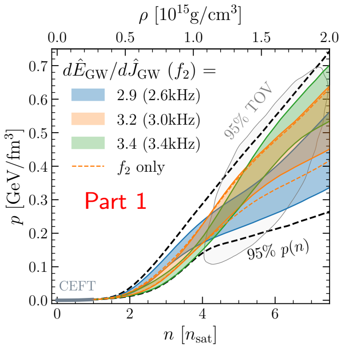


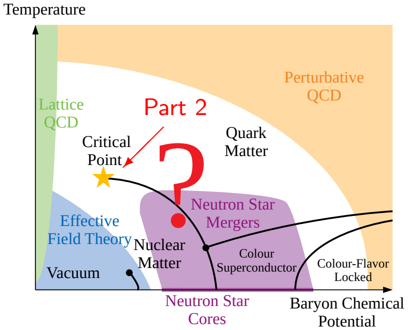

Part 1: EOS constraints from long ringdown slope

# Correlating GWs with EOS properties

- Single most important GW-constraint from **inspiral** part of GW170817

$$\tilde{\Lambda} \lesssim 720 \quad (\tilde{\Lambda} = 384^{+306}_{-158})^* .$$

- Imposed in dense-matter modeling and agnostic-EOS inference studies.
- Next-generation GW facilities will see also **post-merger** part at high SNR.
- Routinely computed via large-scale GRMHD simulations given EOS input.
- **Dominant $f_2$-peak** in post-merger spectrum as typical EOS diagnostic.
- **Mechanism:** stiff EOS give large radii, slow rotation and low frequencies.

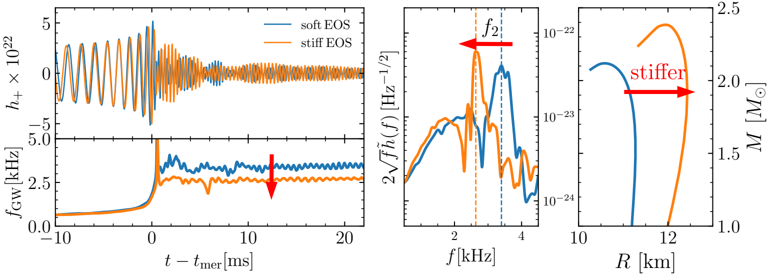


*via physics-informed priors: Magnall, CE, Rezzolla, Lasky, Goode 2504.21526 (ApJL)

# Model-agnostic EOS approach

- **So far:** EOS-GW correlation studies use few "traditional" EOS models.
- However, model-agnostic EOS parametrizations reveal large freedom.
- **Idea:** Large ensemble ($> 10^5$) of generic EOSs that are constrained by astro, nuclear theory and perturbative QCD and cover allowed space.
- **EOS ensemble:** Gaussian process regression method conditioned with Bayesian likelihoods from dense matter theory and astro measurements.

Gorda, Komoltsev, Kurkela 2204.11877 (ApJ)

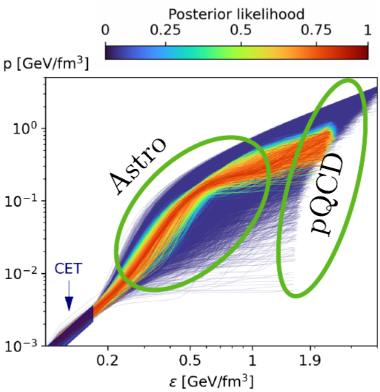


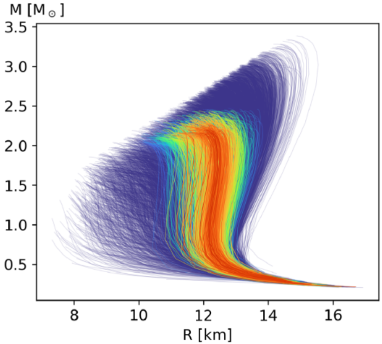

# Golden EOS selection

- **Too many possibilities to simulate:** smart selection recipe is needed.
- Three variables ($M_{\rm TOV}, \mathcal{C}_{\rm TOV}, \ln p_{\rm TOV}$) to characterize the high-density part of the EOS and one ($R_{1.4}$) to break degeneracy at lower densities.
- **Principle component analysis:** 4D distribution essentially 3D-triangular.
- **Six "golden EOSs":** A-E at corners of 68% contours and F in centre.

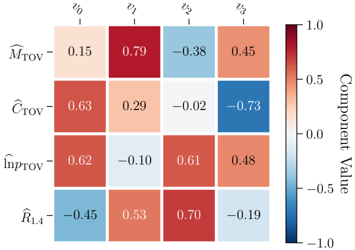


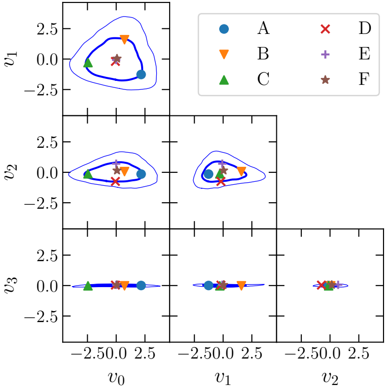

# Golden EOSs and mass-radius relations

- Six EOS models manageable, but **BNS parameter space still huge:** fix $\mathcal{M}_{\mathrm{chirp}} = 1.18\ M_\odot$, but three different mass-ratios $q = \frac{M_1}{M_2} = 0.7, 0.85, 1$.
- Add **$T$-dependence via simple Γ-law approximation** with fixed $\Gamma_{\mathrm{th}} = 1.75$, but analysis remains robust when changing to $\Gamma_{\mathrm{th}} = 1.5, 2.0$.

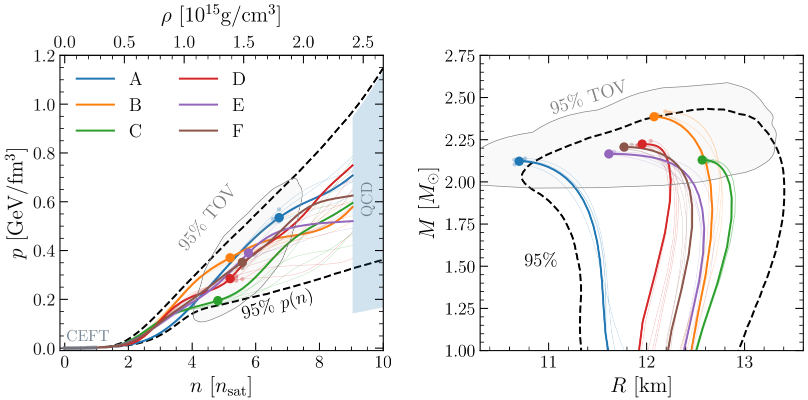

# Emitted GW energy and angular momentum

- Time evolution of GW strain components $h_+, h_\times$ from simulation.
- Emitted energy and angular momentum from post-processing

$$E_{\rm GW}(t) = \frac{r^2}{16\pi}\int_{-\infty}^{t} dt' \left(\dot{h}_+^2 + \dot{h}_\times^2\right) , \; J_{\rm GW}(t) = \frac{r^2}{16\pi}\int_{-\infty}^{t} dt' \left(h_+\dot{h}_\times - \dot{h}_+ h_\times\right) .$$

see, e.g., Bishop, Rezzolla 1606.02532 (Living Reviews in Relativity)

- Useful to normalise with $E_{\rm GW}^{\rm mer} := E_{\rm GW}(t_{\rm mer})$ and $J_{\rm GW}^{\rm mer} := J_{\rm GW}(t_{\rm mer})$.

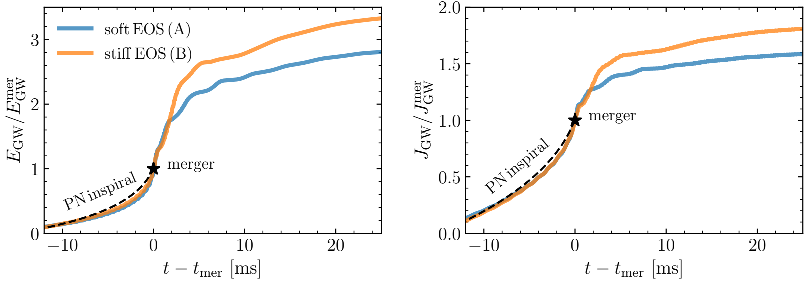


5th-order post-Newtonian Taylor-T2 mode with $\tilde{\Lambda} = 580$ of PyCBC library, Biwer et al 1807.10312 (Publ.Astron.Soc.Pac.)

# Long ringdown

- Post-merger period where $E_{\rm GW}(t)$ and $J_{\rm GW}(t)$ are linearly related.
- Long-ringdown slope numerically close to GW frequency

$$\frac{dE_{\rm GW}}{dJ_{\rm GW}} = \frac{\dot{E}_{\rm GW}}{\dot{J}_{\rm GW}} = \frac{\dot{h}_+^2 + \dot{h}_\times^2}{h_+\dot{h}_\times - \dot{h}_+ h_\times}\,, \qquad f_{\rm GW} = \frac{1}{2\pi}\frac{h_+\dot{h}_\times - \dot{h}_+ h_\times}{h_+^2 + h_\times^2}\,.$$

- Identity for simple quadrupole system with $\ell = 2, m = 2$ deformation:

$$h_+(t) \propto \cos(\phi(t))\,, \quad h_\times(t) \propto \sin(\phi(t))\,, \quad \dot{E}_{\rm GW}/\dot{J}_{\rm GW} = f_{\rm GW}/(2\pi)\,.$$

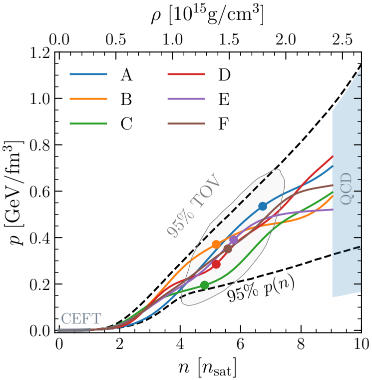


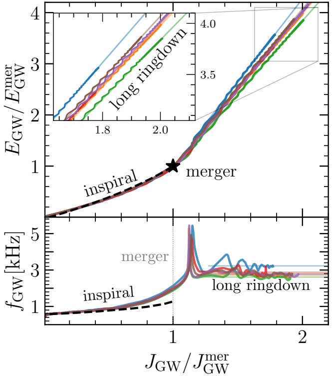

# Robustness

- Waveform dominated by the large-scale deformations of post-merger remnant, only weak influence of small-scale features.
- Essentially no difference between simulations with $200 - 400\ \mathrm{m}$ resolution.
- Also insensitive to approximate thermal effects for $\Gamma_{\mathrm{th}} = 1.5 - 2$.
- However, sensitive to BNS parameters such as chirp mass, but sufficiently different EOSs remain distinguishable.

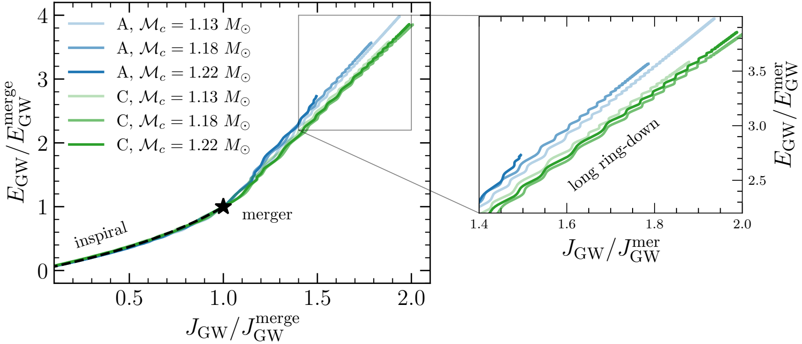

# Correlations

- Slope correlates with maximum neutron star pressure and number density.
- Bilinear fit of simulation data constrains EOS at highest (TOV) densities

$$\frac{d\hat{E}_{\rm GW}}{d\hat{J}_{\rm GW}} = \beta_0 + \beta_1\, p_{\rm TOV} + \beta_2\, n_{\rm TOV} + \beta_3\, q + \beta_4\, q\, p_{\rm TOV} + \beta_5\, q\, n_{\rm TOV} + \beta_6\, p_{\rm TOV}\, n_{\rm TOV}\,.$$

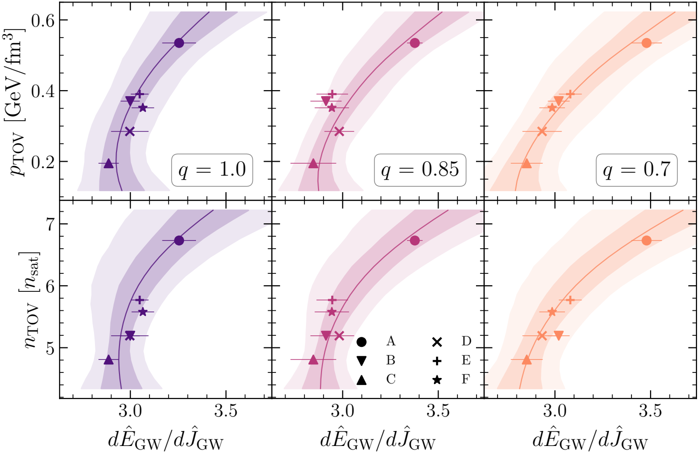

# Impact of slope measurement

- Mock measurement: assume measured values for the slope $d\hat{E}_{\mathrm{GW}}/d\hat{J}_{\mathrm{GW}}$ and $f_2$ with $\pm 4\%$ measurement uncertainty.
- Correlation gives new evidence to update EOS constraints at all densities.
- Slightly improvement compared to measuring just $f_2$.
- Pearson-correlation coefficients slightly larger for $d\hat{E}_{\mathrm{GW}}/d\hat{J}_{\mathrm{GW}}$ than for $f_2$

$$r(dE_{\mathrm{GW}}/dJ_{\mathrm{GW}}, p_{\mathrm{TOV}}) = 0.877 \quad \text{vs} \quad r(f_2, p_{\mathrm{TOV}}) = 0.792\,.$$

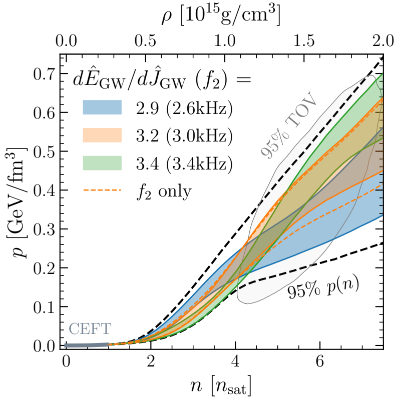


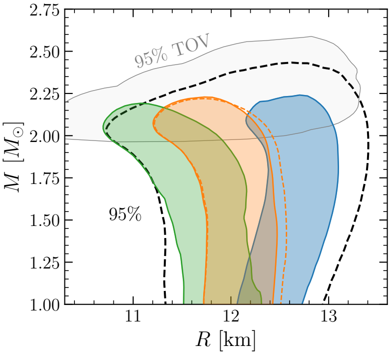

# Summary Part 1

- Looking for EOS-GW correlations in large model-agnostic EOS set.
- Principle component analysis to single out few golden EOSs.
- Correlations between long ringdown slope $d\hat{E}_{\mathrm{GW}}/d\hat{J}_{\mathrm{GW}}$ and $(p_{\mathrm{TOV}}, n_{\mathrm{TOV}})$ constrain the EOS at maximum NS core densities.
- Correlation + Bayes theorem: EOS (MR) constraints at all densities.
- Improvement compared to measuring $f_2$ only.

## Part 2: Critical endpoint inference with V-QCD

# The QCD critical-endpoint hypothesis

- Lattice QCD with physical quark masses shows crossover at $\mu_B = 0$.
- Assuming $1^{st}$-order PT at small $T$ implies existence of critical endpoint.
- Supported by EFT + FRG, but alternatives, e.g., quark-hadron continuity.
- Extensive theoretical and experimental efforts (RHIC BES-II, ...) suggest:

$$\mu_{\text{crit}} \gtrsim 300 - 400 \text{ MeV}$$

The Star Collaboration 2504.00817

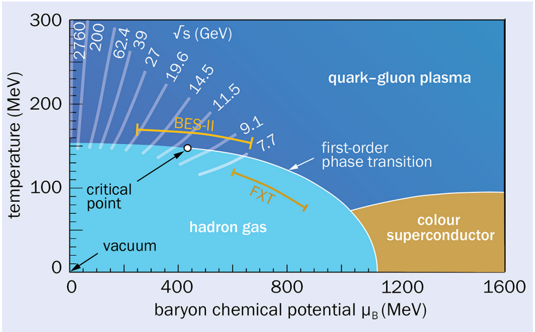


CERNCOURIER (8 July 2025) https://cerncourier.comstar-hunts-qcd-critical-point

Credit: Adapted from L Du et al. 2024 Int. J. Mod. Phys. 33 2430008

# V-QCD hybrid model

- Low density: Steiner-Fisher-Hempel (SFHo) + meson gas at high $T$.
  Steiner, Hempel, Fischer 1207.2184 (APJ)
- Random $c_s^2$-segments to connect crust with cold V-QCD nuclear matter.
  Annala, Gorda, Kurkela, Nättilä, Vuorinen 1903.09121 (Nature Physics)
- Hom. V-QCD baryons and unpaired massless quark matter at $\mu_B > \mu_{\mathrm{PT}}$.
  Ishii, Järvinen, Nijs 1903.06169 (JHEP); Jokela, Jarvinen, Remes 1809.07770 (JHEP);
  Demircik, CE, Järvinen 2112.12157 (PRX)
- Excluded-volume corrected van der Waals model matched at $T = 0$.
  Vovchenko, Motornenko, Alba, Gorenstein, Satarov, Stöcker 1707.09215 (PRC)

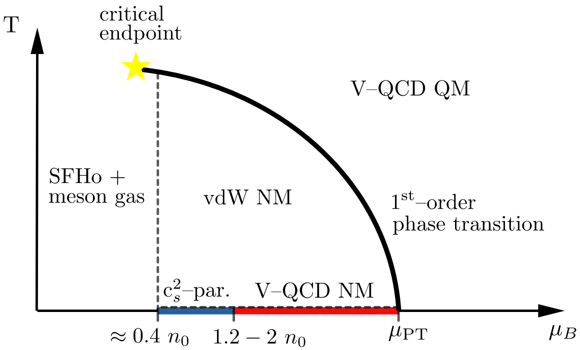

# V-QCD parametrization

- Leading term $W_0$ of the flavor potential in tachyonic DBI action

$$S_{\mathrm{DBI}} \propto \int d^5x\, V_{f0}(\lambda) e^{-\tau^2} \sqrt{-\det[\ldots]}\,, \quad V_{f0}(\lambda) = W_0 + W_1\lambda + \ldots$$

- Exponent of CP-odd potential in Cern-Simons action for baryons

$$S_{\mathrm{CS}} \propto \int \mathrm{Tr}\, V_a(\lambda,\tau)\{\ldots\}\,, \quad V_a(\lambda,\tau) = \exp(-b\tau^2)$$

Ishii, Järvinen, Nijs 1903.06169 (JHEP)

- Three basis solutions of parameter sets {5b, 7a, 8b} with coefficients

$$W_0 = \{1, 2.5, 5.886\}\,, \quad b = \{9.4, 10.5, 31.4\}$$

Jokela, Järvinen, Remes 1809.07770 (JHEP)

- Fitting functions: piecewise constant in $\delta b$ and polar coords. in $\mu T$-plane

$$p_{\mathrm{NM}}(\mu, W_0, \delta b)\,, \quad p_{\mathrm{QM}}(T, \mu, W_0)$$

Note: parametrize relative variation $\delta b \in [-0.02, +0.02]$ around given $b$'s.

- High orders necessary to get number density $n_b$ and sound-speed $c_s^2$ right.
- Huge formulas: translate with Mathematica's CForm to C-code.

# Finite-temperature extension of V-QCD baryons

- Similar to DEJ(DD2-VQCD), but assume $\beta$-equilibrium (fixes $Y_e$).
  Demircik, CE, Järvinen 2112.12157 (PRX)
- Ideal hadron gas: fermions $\{n, \bar{n}, p, \bar{p}, e, \bar{e}\}$, mesons $m_j \leqslant 1\mathrm{GeV}$, photons

$$p_{\mathrm{id}}(T, \{\mu_k\}) = \sum_i p_{\mathrm{FD}}^{(i)}(T, \mu_i, m_i) + \sum_j p_{\mathrm{BE}}^{(j)}(T, m_j) + p_\gamma(T)$$

- Excluded-volume correction to account for vdW forces between nucleons

$$p_{\mathrm{ex}}(T, \{\mu_k\}) = p_{\mathrm{id}}(T, \{\tilde{\mu}_k\}), \quad \tilde{\mu}_i = \mu_i - v_0 p_{\mathrm{ex}}(T, \{\mu_k\})$$

- Matching vdW model to cold baryon EOS; smooth transition to SFHo

$$f_{\mathrm{vdW}}(T, n) = f_{\mathrm{ex}}(T, n) + \Delta f(n), \quad \Delta f(n) = f_{\mathrm{cold}}(n) - f_{\mathrm{ex}}(T = 0, n)$$

- Solve for phase transition number densities independently for each T

$$\mu_{\mathrm{NM}}(T, n_{\mathrm{NM}}^*) = \mu_{\mathrm{QM}}(T, n_{\mathrm{QM}}^*), \quad p_{\mathrm{NM}}(T, n_{\mathrm{NM}}^*) = p_{\mathrm{QM}}(T, n_{\mathrm{QM}}^*)$$

- Critical endpoint where (extrapolated) latent heat vanishes across PT

$$\Delta e(T_{\mathrm{crit}}, \mu_{\mathrm{crit}}) = 0, \quad \Delta e(T, \mu) = e_{\mathrm{QM}}(T, n_{\mathrm{QM}}^*(\mu)) - e_{\mathrm{NM}}(T, n_{\mathrm{NM}}^*(\mu))$$

# Setting up the V-QCD hybrid ensemble

Construct prior from uniformly sampling over free parameters

- V-QCD parameters: $W_0 \in [0, 6]$, $\delta b \in [-0.02, +0.02]$.
- Random monotonic $c_s^2 \in [c^2_{s,\mathrm{SFHo}}, c^2_{s,\mathrm{V-QCD}}]$ between SFHo and V-QCD.
- Marginalize over vdW excluded volume $v_0 \in \{0.56, 0.8, 1.0\}\ \mathrm{fm}^3$.

Consider nuclear theory and astrophysics constraints

- 2NLO CEFT error band for pressure up to $n \approx 2\ n_s$.

  Drischler, Han, Lattimer, Prakash, Reddy, Zhao 2009.06441 (PRC)
- Mass measurements: PSR J1614-2230 ($M = 1.928 \pm 0.017 M_\odot$)
- Combined mass-radius X-ray measurements by NICER

  PSR J0740+6620: $M = 2.08^{+0.07}_{-0.07}\ M_\odot$, $R = 12.39^{+1.30}_{-0.98}\ \mathrm{km}$

  PSR J0030+0451: $M = 1.44^{+0.15}_{-0.14}\ M_\odot$, $R = 13.02^{+1.24}_{-1.06}\ \mathrm{km}$
- Tidal deformability by Ligo/Virgo: $\tilde{\Lambda} = 300^{+420}_{-230}$
- Use Bayes theorem to determine likelihood of each EOS

$$P(\mathrm{EOS}|\mathrm{data}) \propto P(\mathrm{CEFT}|\mathrm{EOS})P(\mathrm{Mass}|\mathrm{EOS})P(\tilde{\Lambda}|\mathrm{EOS})P(\text{X-ray}|\mathrm{EOS})$$

# Constrained cold EOS ensemble

- Posterior of $10^5$ models agrees well with model agnostic results (no PT).
- Predictions at 95% confidence, e.g., for onset density from histograms.

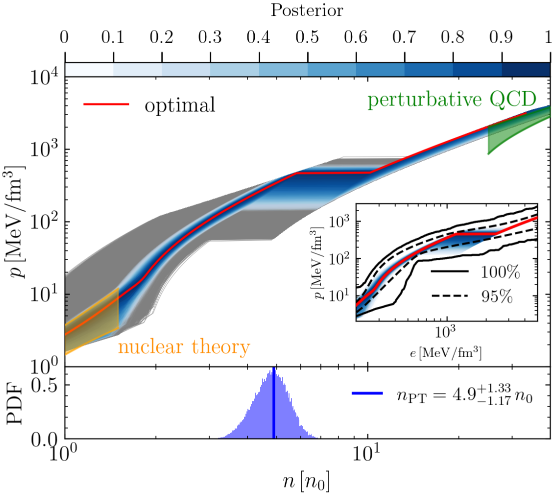

# Cold EOS properties

Estimates for EOS properties from likelihood-weighted histograms.

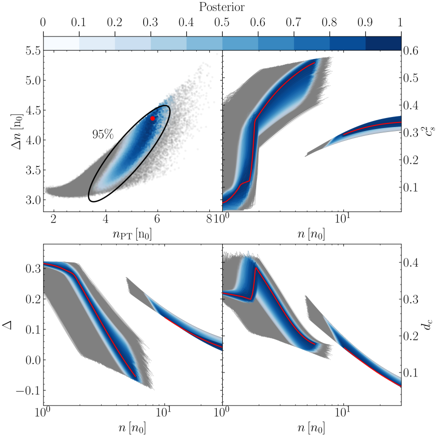


- Onset density and transition strength:

$$n_{\rm PT} = 4.9^{+1.33}_{-1.17}\, n_0\,,\ \ \Delta n_{\rm PT} = 3.75^{+0.70}_{-0.53}\, n_0$$

$$n_{\rm PT}^{\rm opt} = 5.81\ n_0\,,\ \ \Delta n_{\rm PT}^{\rm opt} = 4.36\ n_0$$

- Steep rise of sound-speed before PT:

$$c_s^2 \lesssim 0.6\,,\ \max[c_{s,\rm opt}^2] = 0.55$$

- Conformal anomaly: $\Delta = 1/3 - p/e$
  Fujimoto et al. 2207.06753 (PRL)
  minimum value in NM: $\Delta \approx -0.1$.
- $d_c = \sqrt{\Delta^2 + (\Delta')^2}$, $\Delta' = \mathrm{d}\Delta/\mathrm{d}\log e$
  Annala et al. 2303.11356 (Nature Commun.)

  global max. in NM: $d_c \approx 0.4$ at $n \approx 2\, n_0$
  minimum in NM at PT: $d_c \approx 0.16$
  maximum in QM at PT: $d_c \approx 0.24$

# Static neutron star properties

- Strong first-order transition $\Rightarrow$ no stable quark matter in static stars.
- Mass-radius estimates:

$$R_{1.4} = 12.71^{+0.67}_{-0.66}\,\mathrm{km}\,, \quad M_{\mathrm{TOV}} = 2.22^{+0.20}_{-0.22}\,M_{\odot}\,.$$

- Bounds on binary tidal deformability parameter:

V-QCD: $\tilde{\Lambda}_{1.188} = 586^{+239}_{-175}$ vs. model-agnostic (no PT): $\tilde{\Lambda}_{1.188} = 384^{+306}_{-158}$.

- Smaller error and larger mean value, because specific model with stiff NM.

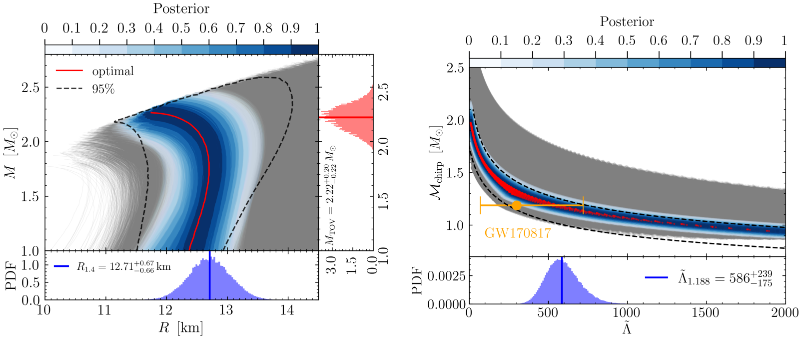

# Phase diagram and critical endpoint estimate

- Results agree well with experimental bound and other theoretical estimates
  $$(\mu_{\text{crit}}, T_{\text{crit}}) = (626^{+91}_{-176}, 119^{+14}_{-6})\,\text{MeV}\,, \quad (\mu^{\text{opt}}_{\text{crit}}, \text{T}^{\text{opt}}_{\text{crit}}) = (683, 116)\ \text{MeV}\,.$$
- Follow trend of lattice extrapolations and 95% CI above freeze-out curve.

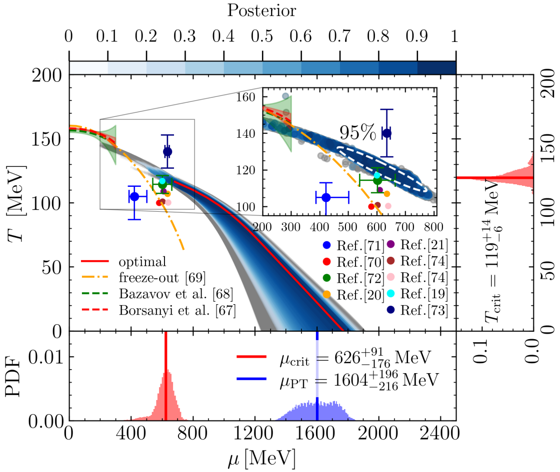

# Summary Part 2

- Large ongoing experimental efforts locating hypothetical critical endpoint.
- Approximate lower bound from HIC experiment: $\mu_{\rm crit} \gtrsim 300 - 400\ \mathrm{MeV}$.
- Idea: derive predictions from astro-constrained V-QCD hybrid ensemble.
- Consistent with experimental bounds; same ball-park as other methods.
- First large-scale Bayesian analysis of V-QCD, however many caveats:
  - No true crossover at small $\mu_{\rm B}$, just extrapolated trend of latent heat.
  - Finite-T part from vdW, not directly from V-QCD baryons.
  - No quark masses, in particular no strange quarks (instabilities!).
  - Only unpaired quark matter, but color superconductor expected.
  - ...
- Conclusion: Bayesian framework to properly apply experimental and observational constrains in holographic models is there, but significant theory improvement necessary - so still a lot of interesting work ahead!